THIELE CENTRE
FOR APPLIED MATHEMATICS IN NATURAL SCIENCE

Time change and universality in turbulence

Ole E. Barndorff-Nielsen and Jürgen Schmiegel

Research Report No. 15 | September 2006

Time change and universality in turbulence

This Thiele Research Report is also Research Report number 484 in the Stochastics Series at Department of Mathematical Sciences, University of Aarhus, Denmark.

Time change and universality in turbulence

Ole E. Barndorff-Nielsen and Jürgen Schmiegel
Thiele Centre for Applied Mathematics in Natural Sciences,
Department of Mathematical Sciences,
University of Aarhus, DK–8000 Aarhus, Denmark *

Abstract

We discuss a unifying description of the probability densities of turbulent velocity increments for a large number of turbulent data sets that include data from low temperature gaseous helium jet experiments, a wind tunnel experiment, an atmospheric boundary layer experiment and a free air jet experiment. Taylor Reynolds numbers range from $R_\lambda = 80$ for the wind tunnel experiment up to $R_\lambda = 17000$ for the atmospheric boundary layer experiment. Empirical findings strongly support the appropriateness of normal inverse Gaussian distributions for a parsimonious and universal description of the probability densities of turbulent velocity increments. Furthermore, the application of a time change in terms of the scale parameter δ of the normal inverse Gaussian distribution results in a collapse of the densities of velocity increments onto Reynolds number independent distributions. We discuss this kind of universality in terms of a stochastic equivalence class that reformulates and extends the concept of Generalized Extended Self-Similarity.

PACS: 47.27.-i
Keywords: Generalized Extended Self-Similarity, hierarchical models, normal inverse Gaussian distribution, stochastic equivalence class, turbulence

*The authors are much indebted to K.R. Sreenivasan, J. Peinke and B. Chabaud for allowing the use of the data sets. J.S. acknowledges support from the Carlsberg Foundation.

1 Introduction

Turbulent flows are expected to reveal universal features in the limit of large Reynolds numbers and for scales within the inertial range [1]. The most prominent example is universal scaling of velocity structure functions [2], expected to hold in the limit of very large Reynolds numbers. To account for small or moderate Reynolds number flows, the concepts of Extended Self-Similarity (ESS) [3, 4] and Generalized Extended Self-Similarity (GESS) [5, 6] have been introduced which considerably extend the scaling range when plotting structure functions of different orders against each other. Recently it has been shown that ESS and GESS are strongly related to hierarchical models introduced by She and Leveque [7]. In fact, it has been shown in [8] that a generalization of the She-Leveque hierarchical structure (SLHS) is equivalent to GESS, thus unifying these basic approaches in turbulence theory.

In this paper we discuss a new type of universality of the probability densities (pdf) of turbulent velocity increments that is not restricted to the large Reynolds number limit and holds equally well for all scales. In a previous study [9] it has been shown that the normal inverse Gaussian (NIG) distribution approximates the pdf of turbulent velocity increments to high accuracy. Moreover, using the estimated scale parameter δ of the approximate NIG distributions as a time change, the densities of velocity increments of different experimental situations and different Reynolds numbers collapse onto Reynolds number independent densities.

In the present study we confirm and further support these empirical findings for many more turbulent data sets. We also investigate the relation of the empirically found inner time change to the statistical properties associated with GESS and SLHS. In particular, we show that the collapse of the densities of turbulent velocity increments onto universal densities can be expressed in terms of a stochastic equivalence class (SEC) which, in turn, is equivalent to GESS and SLHS. In showing this equivalence, we relate and extend GESS and SLHS (originally formulated as statistical properties within one turbulent experiment) to a statistical property relating different turbulent experiments.

Section 2 provides some background material on normal inverse Gaussian distributions that is essential for the analysis of the densities of velocity increments. Section 3 briefly describes the type of data we use for the analysis and Section 4 discusses the analysis of turbulent data within the class of normal inverse Gaussian distributions. Section 5 introduces the concept of an intrinsic inner clock. The relation of the proposed time change to GESS and hierarchical scaling models are discussed in Sections 6 and 7, respectively. Section 8 concludes.

2 The normal inverse Gaussian law

The normal inverse Gaussian law, with parameters α, β, μ and δ, is the distribution on the real axis $\mathbf{R}$ having probability density function

$$p(x;\alpha,\beta,\mu,\delta) = a(\alpha,\beta,\mu,\delta)q\left(\frac{x-\mu}{\delta}\right)^{-1} K_1\left\{\delta\alpha q\left(\frac{x-\mu}{\delta}\right)\right\} e^{\beta x} \qquad (1)$$

where $q(x) = \sqrt{1+x^2}$ and

$$a(\alpha, \beta, \mu, \delta) = \pi^{-1}\alpha \exp\left\{\delta\sqrt{\alpha^2 - \beta^2} - \beta\mu\right\} \tag{2}$$

and where K_1 is the modified Bessel function of the third kind and index 1. The domain of variation of the parameters is given by $\mu \in \mathbf{R}$, $\delta \in \mathbf{R}_+$, and $0 \leq |\beta| < \alpha$. The distribution is denoted by $\mathrm{NIG}(\alpha, \beta, \mu, \delta)$.

If X is a random variable with distribution $\mathrm{NIG}(\alpha, \beta, \mu, \delta)$ then the cumulant generating function of X, i.e. $\mathrm{K}(\theta; \alpha, \beta, \mu, \delta) = \log \mathrm{E}\{e^{\theta X}\}$, has the form

$$\mathrm{K}(\theta; \alpha, \beta, \mu, \delta) = \delta\{\sqrt{\alpha^2 - \beta^2} - \sqrt{\alpha^2 - (\beta+\theta)^2}\} + \mu\theta. \tag{3}$$

It follows immediately from this that if $x_1, \ldots, x_m$ are independent normal inverse Gaussian random variables with common parameters α and β but individual location-scale parameters μ_i and δ_i $(i = 1, \ldots, m)$ then $x_+ = x_1 + \cdots + x_m$ is again distributed according to a normal inverse Gaussian law, with parameters $(\alpha, \beta, \mu_+, \delta_+)$.

Furthermore, the first four cumulants of $\mathrm{NIG}(\alpha, \beta, \mu, \delta)$, obtained by differentiation of (3), are found to be

$$\kappa_1 = \mu + \frac{\delta\rho}{\sqrt{1-\rho^2}}, \quad \kappa_2 = \frac{\delta}{\alpha(1-\rho^2)^{3/2}} \tag{4}$$

and

$$\kappa_3 = \frac{3\delta\rho}{\alpha^2(1-\rho^2)^{5/2}}, \quad \kappa_4 = \frac{3\delta(1+4\rho^2)}{\alpha^3(1-\rho^2)^{7/2}}, \tag{5}$$

where $\rho = \beta/\alpha$. Hence, the standardised third and fourth cumulants are

$$\bar{\kappa}_3 = \frac{\kappa_3}{\kappa_2^{3/2}} = 3\frac{\rho}{\{\delta\alpha(1-\rho^2)^{1/2}\}^{1/2}} \tag{6}$$

and

$$\bar{\kappa}_4 = \frac{\kappa_4}{\kappa_2^2} = 3\frac{1+4\rho^2}{\delta\alpha(1-\rho^2)^{1/2}}. \tag{7}$$

We note that the NIG distribution (1) has semiheavy tails; specifically,

$$p(x; \alpha, \beta, \mu, \delta) \sim \text{const.}\, |x|^{-3/2} \exp\left(-\alpha\,|x| + \beta x\right),\ x \to \pm\infty \tag{8}$$

as follows from the asymptotic relation

$$K_\nu(x) \sim \sqrt{2/\pi}\, x^{-1/2} e^{-x} \quad \text{as} \quad x \to \infty. \tag{9}$$

The normal inverse Gaussian law $\mathrm{NIG}(\alpha, \beta, \mu, \delta)$ has the following important characterisation in terms of the bivariate Brownian motion with drift. Let $B(t) = \{B_1(t), B_2(t)\}$ be a bivariate Brownian motion starting at $(\mu, 0)$ and having drift vector (β, γ) where $\beta \in \mathbf{R}$ and $\gamma \geq 0$. Furthermore, let T denote the time when B_1 first reaches level $\delta > 0$ and let $X = B_2(T)$. Then $X \sim \mathrm{NIG}(\alpha, \beta, \mu, \delta)$ with $\alpha = \sqrt{\beta^2 + \gamma^2}$.

A systematic study of the class of normal inverse Gaussian distributions, and of associated stochastic processes, was begun in [10, 11, 12, 13, 14]. Further theoretical developments and applications are discussed in [15, 16, 17, 18, 19, 20, 21, 22, 23, 24, 25, 26, 27, 28]. As discussed in the papers cited and in references given there, the class of NIG distributions and processes have been found to provide accurate modelling of a great variety of empirical findings in the physical sciences and in financial econometrics. (The wider class of generalised hyperbolic distributions, introduced in [29], provides additional possibilities for realistic modelling of dynamical processes, see references in the papers cited above.)

3 Description of the data

The data sets we analysed consist of one-point time records of the longitudinal (along the mean flow) velocity component. The data are from the atmospheric boundary layer (data set (at)) [30, 31], from a gaseous helium jet flow (data sets (h85)–(h1181)) [32], from a free air jet experiment (data set (f)) [33] and from a wake generated by a flat plate (data set (w)) [34]. This collection of data sets comprise a wide range of Reynolds numbers from 80 (w) up to 17000 (at). Table 1 lists the Taylor Reynolds numbers R_λ. We refer to [30, 31, 32, 33, 34] for more information about the data sets.

We perform the statistical analysis of the densities of velocity increments u in terms of temporal statistics

$$u_s = v(t+s) - v(t) \tag{10}$$

where $v(t)$ denotes the longitudinal velocity component at time t. Note that we do not invoke Taylor's Frozen Flow Hypothesis which translates (10) into spatial scales $u(x) = u(x-l) - u(x)$ (reversing the sign of the usual definition of spatial velocity increments) where $l = \bar{v}s$ and $\bar{v}$ denotes the mean velocity. Defining velocity increments u_s according to (10), we expect the skewness of the distribution of velocity increments to be positive.

We furthermore normalized each data set by its standard deviation, i.e. the variance of each velocity time series is one.

4 Distribution of velocity increments

Figure 1 shows the densities of timewise velocity increments (10) for different data sets and various time scales s (in units of the finest resolution). The solid lines denote the approximation of the densities within the class of NIG distributions using maximum likelihood estimation of the four parameters α, β, δ and μ of the NIG distribution. The NIG distributions fit the empirical densities to high accuracy for all amplitudes u. The same high quality of the fit holds for all scales (not shown here). We performed the same analysis for all data sets that are listed in Table 1 and obtained similar plots for all lags s and all amplitudes u (not shown here).

For each data set the approximation within the class of NIG distributions is completely described by the four parameter sets $\alpha(s)$, $\beta(s)$, $\delta(s)$ and $\mu(s)$ as functions

of the time scale s. Due to the stationarity of the velocity signal we are able to express one of them, say $\mu(s)$ in terms of the other three parameter sets. Stationarity implies zero mean for velocity increments. In terms of the parameters of the NIG distributions we get from (4)

$$\mu(s) = -\frac{\delta(s)\beta(s)}{\sqrt{\alpha^2(s) - \beta^2(s)}}. \tag{11}$$

Thus, for each data set, we are left with three parameter sets to fully describe the evolution of the densities of velocity increments across scales. To reduce the scatter of the different parameters as a function of the scale s we introduce as new parameters the set δ, α/δ and

$$\xi = \left(1 + \delta\sqrt{\alpha^2 - \beta^2}\right)^{-1/2}. \tag{12}$$

The parameter ξ is called the steepness parameter of the NIG distribution and it plays a role similar to the standardized fourth order cumulant.

Figure 2 shows the estimated scale parameters $\delta(s)$ of the approximate NIG distributions as a function of the lag s. Note, in particular, that the scale parameter δ is monotonically increasing with the time scale s for all data sets.

Figures 3(a) and 4(a) show the estimated parameters $\alpha(s)/\delta(s)$ and $\xi(s)$, respectively. The functional dependence of the parameters of the approximate NIG distributions on the scale s changes substantially with the Reynolds number and the experimental conditions.

Figures 3(b) and 4(b) show the estimated parameters $\alpha(s)/\delta(s)$ and $\xi(s)$ as a function of the estimated scale parameter $\delta(s)$, respectively. For both of the two parameter sets there is a striking collapse onto one single curve. Note that the various data sets cover a wide range of Reynolds numbers and widely different experimental situations. It is the scale parameter $\delta(s)$ that describes the individual characteristics of each data set, but in terms of $\delta(s)$ the remaining parameters show a universal behaviour, independent of the experimental set up and independent of the Reynolds number.

5 Time change and universality

The collapse of the parameters $\alpha(s)/\delta(s)$ and $\xi(s)$ of the different data sets onto single, apparently universal curves when plotted as a function of the scale parameter $\delta(s)$ immediatedly implies a collapse of the corresponding densities of velocity increments.

Figure 5 shows a collection of densities of velocity increments that correspond to fixed values of the scale parameter δ. As expected from Figures 3(b) and 4(b) the densities collapse onto Reynolds number independent distributions that are solely labeled by the scale parameter δ.

In other words, the densities of velocity increments of the type of data we analyzed in this paper follow a one-parameter curve in the space of probability densities.

Each individual data set covers a certain part of this one-parameter curve. The parameter δ of the corresponding approximation of the densities within the class of NIG distribution is a very good approximation of this characteristic parameter.

The change from scale s to $\delta(s)$ in the labeling of the densities of velocity increments corresponds to a time change such that individual characteristics of each data set are covered by the functional dependence of $\delta(s)$ but in terms of which the densities behave in a universal fashion. The intrinsic time change we propose here applies equally well to all scales, providing a unified description of dissipative, inertial and sup-inertial scales.

Of course, any statistical quantity that monotonically increases with the time scale s is equally well suited for being a universal time change. In particular, the variance of velocity increments increases with increasing time scale s and, as such, may serve as a time change. However, using the scale parameter $\delta(s)$ of the approximate NIG distributions seems to be more appropriate since it directly relates to the parameters of the densities of velocity increments.

The collapse of the densities of velocity increments can be put into more mathematical terms by introducing a stochastic equivalence class of the form

$$\frac{u_{s_1}^{(i)}}{g^{(i)}(s_1)} \stackrel{d}{=} \frac{u_{s_2}^{(j)}}{g^{(j)}(s_2)} \;\Leftrightarrow\; F^{(i)}(s_1) = F^{(j)}(s_2) \tag{13}$$

where $\stackrel{d}{=}$ denotes equality in distribution and the superscripts (i) and (j) label the different data sets. The monotonic functions F denote the intrinsic time changes and the deterministic functions g are introduced here to account for more general situations (see the next Section).

In the present analysis of the data sets in Table 1 we have

$$g^{(i)}(s) = \sqrt{\mathrm{Var}(v^{(i)})}, \tag{14}$$

independent of s, i.e. the functions g reduce to a constant normalization. Here Var denotes the variance. For the intrinsic time change F we obtain from our analysis within the class of NIG distributions

$$\delta^{(i)}(s) = F^{(i)}(s) \tag{15}$$

to high accuracy.

In more general situations (i.e. anisotropic flows, see next Section), the function $g^{(i)}(s)$ can, in principle, be estimated using cumulants of order two and four. For that we choose a reference experiment (j) and arbitrarily set $g^{(j)}(s) \equiv 1$. From (13) we get

$$(g^{(i)}(s_1))^2 = \frac{c_2(u^{(i)}(s_1))}{c_2(u^{(j)}(s_2))} \tag{16}$$

and

$$(g^{(i)}(s_1))^4 = \frac{c_4(u^{(i)}(s_1))}{c_4(u^{(j)}(s_2))} \tag{17}$$

where s_1 and s_2 are the corresponding time scales where the densities of velocity increments at time scale s_1 of experiment (i) and time scale s_2 of experiment (j)

collapse. Here c_n denotes the cumulant of order n. Combining (16) with (17) gives

$$\frac{c_4(u^{(i)}(s_1))}{(c_2(u^{(i)}(s_1)))^2} = \bar{c}_4(u^{(i)}(s_1)) = \bar{c}_4(u^{(j)}(s_2)) \tag{18}$$

where $\bar{c}_4$ denotes the standardized fourth order cumulant. From (18) the corresponding time scales s_1 and s_2 can be estimated and, using (16), the function $g^{(i)}$ is determined (relative to the function $g^{(j)}$).

6 Time change and Generalized Extended Self-Similarity

This Section examines the relation between the stochastic equivalence class (SEC) proposed in (13) and the concept of Extended Self-Similarity (ESS) and its generalization to Generalized Extended Self-Similarity (GESS). We will show that under mild conditions the SEC approach is equivalent to GESS when $g(s)$ depends on the scale s and SEC is equivalent to ESS when $g(s)$ does not depend on the scale s.

The concept of GESS [5, 6] can be expressed (in the time domain, invoking Taylor's Frozen Flow Hypothesis) as

$$S_n(s) = G_n g_1(s)^n g_2(s)^{\xi(n)} \tag{19}$$

where $g_1(s)$ and $g_2(s)$ are scale-dependent functions and $\xi(n)$ is an exponent independent of scale. The constants G_n are assumed to be universal. The structure functions $S_n(s)$ are defined as the moments of velocity increments of order n

$$S_n(s) = \mathrm{E}\left\{u(s)^n\right\}$$

where $\mathrm{E}\{\cdot\}$ denotes the expectation.

A stronger statement is given by ESS [3, 4] which may be written as

$$S_n(s) = G_n G^n g_2(s)^{\xi(n)} \tag{20}$$

where G is a velocity scale. ESS corresponds to GESS for $g_1(s) = G =$ constant.

ESS and GESS hold for scales s that considerably extend the inertial range. While ESS applies to a wide range of isotropic flows, it is of limited use in anisotropic flows. This inspired the study of GESS which equally well applied to anisotropic flows.

For the comparison of SEC with ESS and GESS we will refer to another basic concept in turbulence, the existence of a fully developed turbulent flow (FDT) characterized as a turbulent state where scaling of structure functions of all orders n holds within the inertial range (assumed to be very large)

$$S_n(s) = G_n G^n \left(\frac{s}{T}\right)^{\xi(n)}, \tag{21}$$

where T is some reference time scale.

The scaling relation (21) corresponds to GESS with

$$g_1(s) = G \tag{22}$$

and

$$g_2(s) = \frac{s}{T}. \tag{23}$$

In its original formulation, ESS and GESS refer to spatial scales. Here we restrict ourselves to purely temporal statistics and reformulate ESS and GESS in the time domain, using Taylor's Frozen Flow Hypothesis. This reformulation is naturally adapted to our data sets consisting of time series at a fixed spatial position.

It has been shown in [9] that SEC together with (14) implies ESS under the assumption of FDT. On the other hand, if the distribution of velocity increments is determined by all its finite moments then ESS and the assumption of FDT implies SEC. Here we supplement these results by showing that SEC with a given function $g(s)$ and FDT implies GESS with universal exponents $\xi(n)$. Moreover, if the distribution of velocity increments is determined by all its finite moments then GESS and the assumption of FDT implies SEC.

As a first step, we prove that SEC together with FDT implies GESS. Let SEC hold for some arbitrary flow (i) and let (j) be a fully developed turbulent flow which obeys SEC. We denote by $\bar{F}$ the inverse of F (which exists since F is assumed to be monotonic).

It follows from (13) and (21) that

$$S_n^{(i)}(s) = G_n \left(\frac{G^{(j)} g^{(i)}(s)}{g^{(j)}(\bar{F}^{(j)}(F^{(i)}(s)))} \right)^n \left(\frac{\bar{F}^{(j)}(F^{(i)}(s))}{T^{(j)}} \right)^{\xi(n)}. \tag{24}$$

We identify

$$g_1^{(i)}(s) = \frac{G^{(j)} g^{(i)}(s)}{g^{(j)}\left(\bar{F}^{(j)}\left(F^{(i)}(s)\right)\right)} \tag{25}$$

and

$$g_2^{(i)}(s) = \frac{\bar{F}^{(j)}\left(F^{(i)}(s)\right)}{T^{(j)}}. \tag{26}$$

Inserting (25) and (26) in (24) immediatedly establishes the GESS relation (19) for experiment (i). Therefore, SEC and FDT imply GESS with universal exponents $\xi(n)$.

To show that the definitions of the functions g_1 in (25) and g_2 in (26) do not depend on the fully developed turbulent reference state (j), we apply equations (25) and (26) to yet another fully developed turbulent state, say (k), and get, using (22) and (23),

$$g_1^{(k)}(s) = G^{(k)} = \frac{G^{(j)} g^{(k)}(s)}{g^{(j)}\left(\bar{F}^{(j)}\left(F^{(k)}(s)\right)\right)} \tag{27}$$

and

$$g_2^{(k)}(s) = \frac{s}{T^{(k)}} = \frac{\bar{F}^{(j)}\left(F^{(k)}(s)\right)}{T^{(j)}}. \tag{28}$$

Consequently, we have

$$g_1^{(i)}(s) = \frac{G^{(j)}g^{(i)}(s)}{g^{(j)}\left(\bar{F}^{(j)}\left(F^{(i)}(s)\right)\right)} = \frac{G^{(j)}g^{(i)}(s)}{g^{(j)}\left(\bar{F}^{(j)}(F^{(k)}(\bar{F}^{(k)}\left(F^{(i)}(s)\right))\right)}$$
$$= \frac{G^{(k)}g^{(i)}(s)}{g^{(k)}\left(\bar{F}^{(k)}\left(F^{(i)}(s)\right)\right)} \tag{29}$$

and

$$g_2^{(i)}(s) = \frac{\bar{F}^{(j)}\left(F^{(i)}(s)\right)}{T^{(j)}} = \frac{\bar{F}^{(j)}(F^{(k)}(\bar{F}^{(k)}\left(F^{(i)}(s)\right)))}{T^{(j)}}$$
$$= \frac{\bar{F}^{(k)}\left(F^{(i)}(s)\right)}{T^{(k)}}. \tag{30}$$

Equations (29) and (30) are equivalent to (25) and (26) and prove that the expressions (25) and (26) do not depend on the fully developed turbulent reference state (j).

We now prove that GESS together with FDT implies SEC. For that, let GESS hold true for the flows (i) and (k) and let the distribution of velocity increments of the flows (i) and (k) be completely decribed by all their finite moments. Let, again, (j) denote a fully developed turbulent flow obeying (21), (22) and (23). It follows from (19) and (21) that

$$\frac{S_n^{(i)}(s)}{(g_1^{(i)}(s))^n} = \frac{S_n^{(j)}(g_2^{(i)}(s)T^{(j)})}{(G^{(j)})^n} \tag{31}$$

and

$$\frac{S_n^{(k)}(s)}{(g_1^{(k)}(s))^n} = \frac{S_n^{(j)}(g_2^{(k)}(s)T^{(j)})}{(G^{(j)})^n}. \tag{32}$$

We identify

$$g^{(i)}(s) = g_1^{(i)}(s) \tag{33}$$
$$g^{(k)}(s) = g_1^{(k)}(s) \tag{34}$$

and

$$F^{(i)}(s) = g_2^{(i)}(s) \tag{35}$$
$$F^{(k)}(s) = g_2^{(k)}(s) \tag{36}$$

and get from a comparison of (31) and (32)

$$\frac{S_n^{(i)}(s_1)}{g^{(i)}(s_1)^n} = \frac{S_n^{(k)}(s_2)}{g^{(k)}(s_2)^n} \Leftrightarrow F^{(i)}(s_1) = F^{(k)}(s_2). \tag{37}$$

Since the distributions of $u_s^{(i)}$ and $u_s^{(k)}$ are assumed to be defined by all their finite moments, (37) is equal to equality in distribution, i.e. SEC holds for experiments (i) and (k).

This completes the proof that GESS together with FDT and the assumption of the distribution of velocity increments being completely described by all its finite moments implies SEC.

Our empirical analysis showed that $g^{(i)}(s) = \text{constant}$, which corresponds to the ESS case (see (33)). In fact, the experiments we analyzed are isotropic flows for which ESS holds true. For anisotropic flows the normalization $g^{(i)}(s)$ depends on the time scale s in correspondence with the GESS relation (19).

Originally, GESS and ESS express distributional properties of single turbulent experiments. The innovative view of GESS and ESS in terms of SEC provides a much broader interpretation. The scaling functions $g_2(s)$ serve as intrinsic time changes in terms of which the normalized velocity increments, normalized by $g_1(s)$, are universal. Thus GESS and ESS, under the assumption of FDT, turn out to express distributional properties relating different turbulent experiments.

7 Time change and hierarchical structures

The functions g_1 and g_2 in (19) are not unique. However, [8] gives an interpretation of the functions g_1 and g_2 within the famous model of hierarchical structure of She and Leveque [7]. The identification

$$g_1(r) = \mathrm{S}^{(\infty)}(r) \tag{38}$$

and

$$g_2(r) = \frac{\mathrm{S}_3(r)}{[\mathrm{S}^{(\infty)}(r)]^3} \tag{39}$$

associates to $g_1(r)$ the r dependence of the strongest fluctuations and to $g_2(r)$ the normalized r dependence of (typical) weak fluctuations. Here, the strongest fluctuations are characterized by the finite limit

$$S^{\infty}(r) \equiv \lim_{p\to\infty} \frac{S_{p+1}(r)}{S_p(r)}$$

Within the hierarchical framework, the normalization $g^{(i)}$ of velocity increments in (13) is defined in terms of the strongest fluctuations (compare (38) with (33)) and the time change F is defined solely in terms of the weak fluctuations (compare (39) with (35)). Consequently, if the strongest fluctuations do not depend on r, we arrive at $g^{(i)}(r) = \text{constant}$. Furthermore, typical weak fluctuations serve as the intrinsic time change. All in all, SEC states that velocity increments normalized by the strongest fluctuations obey a stochastic equivalence class with an intrisic time change governed by typical weak fluctuations.

8 Conclusions

The proposed stochastic equivalence class constitutes a reformulation and substantially new interpretation of the concept of GESS. We showed that, under a mild moment condition on the distribution of velocity increments and the existence of a fully developed turbulent state, GESS is equivalent to SEC. The equivalence of GESS (and its special case ESS) and the model of hierarchical structure has already been discussed in [8]. The interpretation of GESS in terms of SEC is not merely

a reformulation but a strong extension since SEC combines the statistics of different experiments and different Reynolds numbers while GESS is restricted to the statistical description within one experimental situation. We strongly believe that this innovative view of SEC will find various applications since it allows to directly compare statistical properties of different flows.

The equivalence of SEC and GESS is based on the additional hypothesis of FDT which is generally accepted in turbulence research as being the high Reynolds number limit.

In this paper we empirically verified SEC for a class of data sets where the function g is constant (the ESS case). The empirical study of SEC for a scale dependent function $g(s)$ is currently in progress and will be published elsewhere.

References

[1] U. Frisch (1995), Turbulence. The Legacy of A.N. Kolmogorov. Cambridge University Press, Cambridge, 1995.

[2] K.R. Sreenivasan, R.A. Antonia, Ann. Rev. Fluid Mech. 29 (1997) 435.

[3] R. Benzi, S. Ciliberto, R. Trippiccione, C. Baudet, F. Massaioli, S. Succi, Phys. Rev. E 48 (1993) R29.

[4] R. Benzi, S. Ciliberto, C. Baudet, G.R. Chavarria, R. Tripiccione, Europhys. Lett. 24 (1993) 275.

[5] R. Benzi, L. Biferale, S. Ciliberto, M.V. Struglia, R. Trippiccione, Europhys. Lett. 32 (1995) 709.

[6] R. Benzi, L. Biferale, S. Ciliberto, M.V. Struglia, R. Trippiccione, Physica D 96 (1996) 162.

[7] Z.S. She, E. Leveque, Phys. Rev. Lett. 72 (1994) 336.

[8] E.S.C. Ching, Z.S. She, W. Su, Z. Zou, Phys. Rev. E 66 (2002) 066303.

[9] O.E. Barndorff-Nielsen, P. Blæsild, J. Schmiegel, Eur. Phys. J. B. 41 (2004) 345.

[10] O.E. Barndorff-Nielsen, Research Report 300, Dept. Theor. Statistics, Aarhus University 1995.

[11] O.E. Barndorff-Nielsen, Scand. J. Statist. 24 (1997) 1.

[12] O.E. Barndorff-Nielsen, in Probability Towards 2000. Proceedings of a Symposium held 2-5 October 1995 at Columbia University, edited by L. Acccardi, C.C. Heyde, Springer, New York 1998.

[13] O.E. Barndorff-Nielsen, Finance and Stochastics 2 (1998) 41.

[14] O.E. Barndorff-Nielsen, Theory Prob. Its Appl. 45 (1998) 175.

[15] T.H. Rydberg, Comm. Statist.: Stochastic Models 13 (1997) 887.

[16] T.H. Rydberg, Math. Finance 9 (1999) 183.

[17] K. Prause, Ph.D. Thesis, Albert-Ludwigs-Universität, Freiburg i. Br. 1999.

[18] E. Eberlein, in Lévy Processes – Theory and Applications, edited by O.E. Barndorff-Nielsen, T. Mikosch, S. Resnick, Birkhäuser, Boston 2000.

[19] S. Raible, Ph.D. Thesis, Albert-Ludwigs-Universität, Freiburg i. Br. 2000.

[20] O.E. Barndorff-Nielsen, N. Shephard, J. R. Statist. Soc. B 63 (2001) 167.

[21] O.E. Barndorff-Nielsen, N. Shephard, in Lévy Processes - Theory and Applications, edited by O.E. Barndorff-Nielsen, T. Mikosch, S. Resnick, Birkhäuser, Boston 2001.

[22] O.E. Barndorff-Nielsen, N. Shephard, Scand. J. Statist. 30 (2002) 277.

[23] O.E. Barndorff-Nielsen, K. Prause, Finance and Stochastics 5 (2001) 103.

[24] O.E. Barndorff-Nielsen, S.Z. Levendorskiĭ, Quantitative Finance 1 (2001) 318.

[25] S. Asmussen, J. Rosinski, J. Appl. Probab. 38 (2001) 482.

[26] R. Cont, P. Tankov, Financial Modelling With Jump Processes, Chapman & Hall/CRC, London 2004.

[27] L. Forsberg, On the Normal Inverse Gaussian distribution in Modelling Volatility in the Financial Markets, Acta Universitatis Upsaliemsis, Studia Statistica Upsaliensia 5, Uppsala 2002.

[28] A.J. McNeil, R. Frey, P. Embrechts, Quantitative Risk Management, Princton University Press, Princeton 2005.

[29] O.E. Barndorff-Nielsen, Proc. R. Soc. London A 353 (1977) 401.

[30] B. Dhruva, PhD Thesis, Yale University 2000.

[31] K.R. Sreenivasan, B. Dhruva, Prog. Theor. Phys. Suppl. 130 (1998) 103.

[32] O. Chanal, B. Chebaud, B. Castaing, B. Hébral, Eur. Phys. J. B 17 (2000) 309.

[33] C. Renner, J. Peinke, R. Friedrich, J. Fluid Mech. 433 (2001) 383.

[34] R.A. Antonia, B.R. Pearson, Phys. Rev. E 62 (2000) 8086.

data set	(at)	(f)	(w)	(h85)	(h89)	(h124)	(h208)	(h209)
R_λ	17000	190	80	85	89	124	208	209
data set	(h283)	(h352)	(h463)	(h703)	(h885)	(h929)	(h985)	(h1181)
R_λ	283	352	463	703	885	929	985	1181

Table 1: Taylor Reynolds numbers R_λ for the 16 data sets.

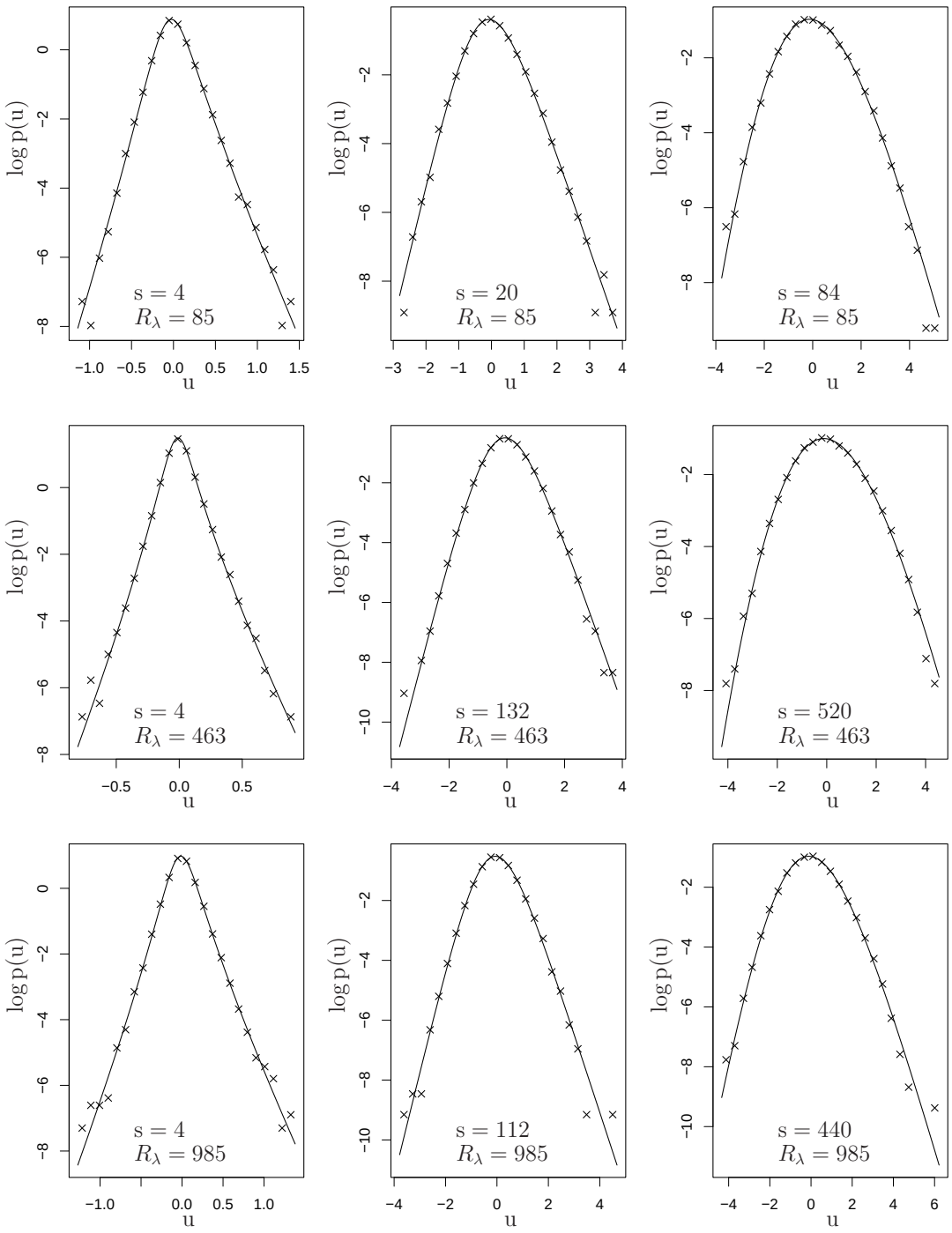

Figure 1: Approximation of the probability densities p of velocity increments within the class of NIG distributions for data sets h85, h463, h985 and lags $s = 4, 20, 84$, $s = 4, 132, 520$ and $s = 4, 112, 440$ (in units of the finest resolution $1/f$, where f denotes the sampling frequency), respectively.

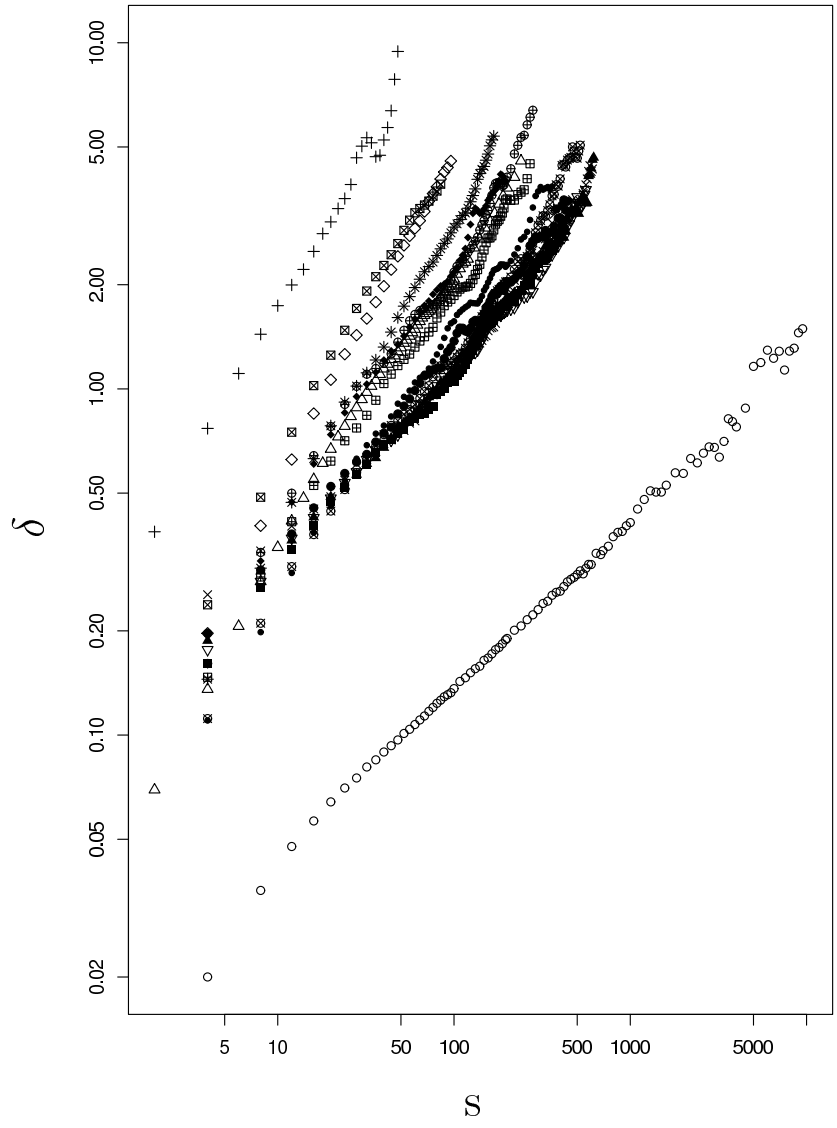

Figure 2: Estimated parameter δ as a function of the lag s (in units of the finest resolution and in double logarithmic representation) for data set (at) ($\circ$), (f) ($\triangle$), (w) ($+$), (h85) ($\boxtimes$), (h89) ($\Diamond$), h124) ($*$), (h208) ($\blacklozenge$), (h209) ($\oplus$), (h283) ($\bullet$), (h352) ($\boxplus$), (h463) ($\otimes$), (h703) ($\times$), (h885) ($\blacksquare$), (h929) ($\triangledown$), (h985) ($\bullet$), (h1181) ($\blacktriangle$).

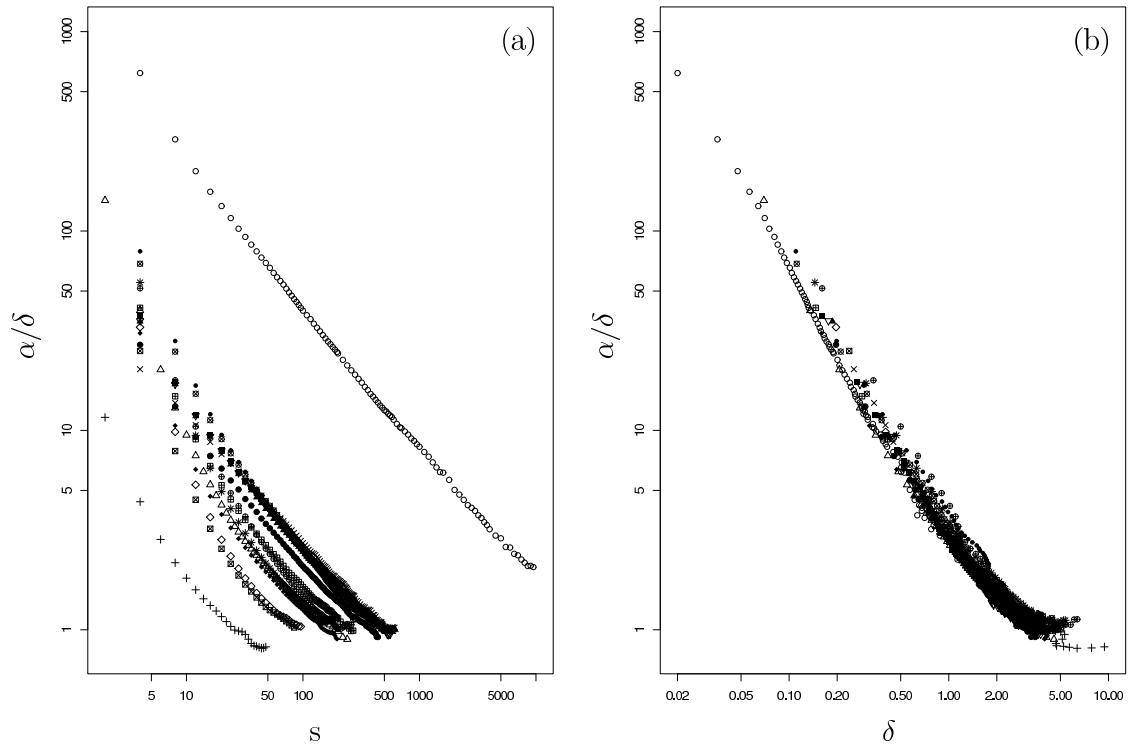

Figure 3: (a) Comparison of $(\alpha/\delta)(s)$ as a function of the lag s (in units of the finest resolution) with (b) $(\alpha/\delta)(\delta)$ as a function of the scale parameter δ in double logarithmic representation. Data sets and symbols correspond to those in Figure 2.

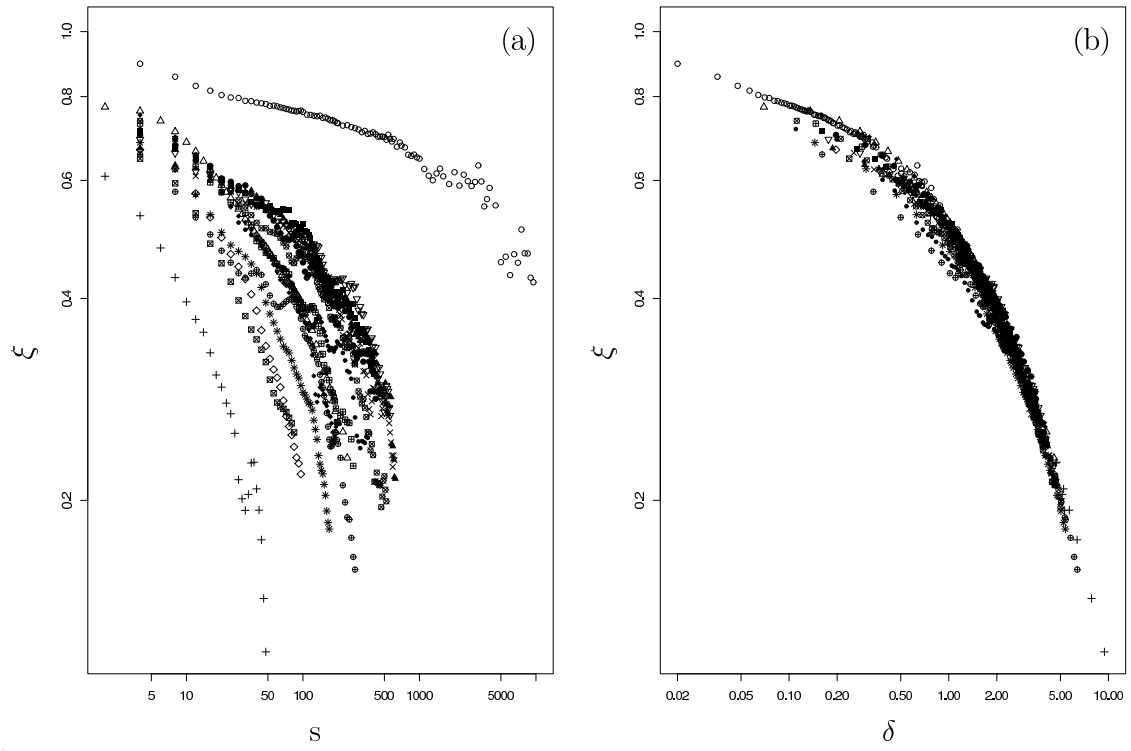

Figure 4: (a) Comparison of $\xi(s)$ as a function of the lag s (in units of the finest resolution) with (b) $\xi(\delta)$ as a function of the scale parameter δ in double logarithmic representation. Data sets and symbols correspond to those in Figure 2.

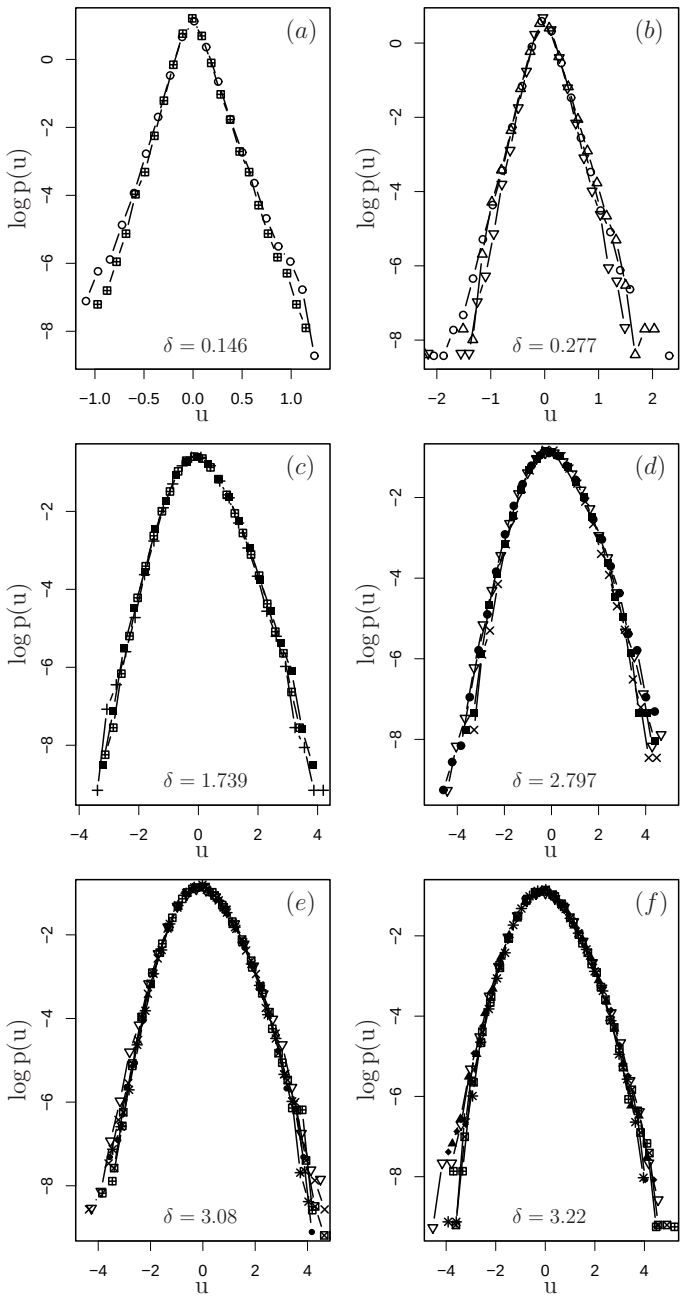

Figure 5: Collapse of the densities $p(u)$ for various fixed values of the scale parameter $\delta(s)$. The corresponding values of the lag s (in units of the finest resolution of the corresponding data set) and the data sets are (a) $(s = 116, \mathrm{at})$ $(\circ)$, $(s = 4, \mathrm{h352})$ $(\boxplus)$, (b) $(s = 440, \mathrm{at})$ $(\circ)$, $(s = 8, \mathrm{f})$ $(\triangle)$, $(s = 8, \mathrm{h929})$ $(\triangledown)$, (c) $(s = 192, \mathrm{h885})$ $(\blacksquare)$, $(s = 88, \mathrm{h352})$ $(\boxplus)$, $(s = 10, \mathrm{w})$ $(+)$, (d) $(s = 380, \mathrm{h885})$ $(\blacksquare)$, $(s = 410, \mathrm{h929})$ $(\triangledown)$, $(s = 350, \mathrm{h703})$ $(\times)$, $(s = 340, \mathrm{h985})$ $(\bullet)$, (e) $(s = 420, \mathrm{h703})$ $(\times)$, $(s = 440, \mathrm{h929})$ $(\triangledown)$, $(s = 180, \mathrm{h352})$ $(\boxplus)$, $(s = 270, \mathrm{h283})$ $(\bullet)$, $(s = 108, \mathrm{h124})$ $(*)$, $(s = 56, \mathrm{h85})$ $(\boxtimes)$, (f) $(s = 470, \mathrm{h929})$ $(\triangledown)$, $(s = 116, \mathrm{h124})$ $(*)$, $(s = 60, \mathrm{h85})$ $(\boxtimes)$, $(s = 188, \mathrm{h352})$ $(\boxplus)$, $(s = 470, \mathrm{h1181})$ $(\blacktriangle)$, $(s = 140, \mathrm{h208})$ $(\blacklozenge)$.